Atmospheric
Chemistry
and Physics
Discussions

1   **The role of H₂SO₄-NH₃ anion clusters in ion-induced aerosol nucleation**

2   **mechanisms in the boreal forest**

3   Chao Yan[1], Lubna Dada[1], Clémence Rose[1], Tuija Jokinen[1], Wei Nie[1,2], Siegfried Schobesberger[1,3] ,

4   Heikki Junninen[1, 4], Katrianne Lehtipalo[1], Nina Sarnela[1], Ulla Makkonen[5], Olga Garmash[1],

5   Yonghong Wang[1], Qiaozhi Zha[1], Pauli Paasonen[1], Federico Bianchi[1], Mikko Sipilä[1], Mikael Ehn[1],

6   Tuukka Petäjä[1,2], Veli-Matti Kerminen[1], Douglas R. Worsnop[1,6], Markku Kulmala[1,2,7]

7

8   [1] Institute for Atmospheric and Earth System Research / Physics, Faculty of Science, University of Helsinki,
9   00560 Helsinki, Finland
10   [2] Joint International Research Laboratory of Atmospheric and Earth System Sciences, School of
11   Atmospheric Sciences, Nanjing University, Nanjing, 210046, P.R. China
12   [3] Department of Applied Physics, University of Eastern Finland, 70211 Kuopio, Finland
13   [4] Institute of Physics, University of Tartu, Ülikooli 18, EE-50090 Tartu, Estoni
14   [5] Finnish Meteorological Institute, 00560 Helsinki, Finland.
15   [6] Aerodyne Research, Inc., Billerica, MA 01821, USA
16   [7] Aerosol and Haze Laboratory, Beijing Advanced Innovation Center for Soft Matter Science and
17   Engineering, Beijing University of Chemical Technology, Beijing, 100029, P.R. China

18   Correspondence to: Chao Yan (chao.yan@helsinki.fi)

19   **Abstract**

20   New particle formation (NPF) provides a large source of atmospheric aerosols, which affect the

21   climate and human health. Ion-induce nucleation (IIN) has been discovered as an important pathway

22   of forming particles within recent chamber studies, however, atmospheric investigation remains

23   incomplete. For this study, we investigated the air anion compositions in the boreal forest in Southern

24   Finland for 3 consecutive springs, with a special focus on H_2SO_4-NH_3 anion clusters. We found that

25   the ratio between the concentrations of highly oxygenated organic molecules (HOMs) and H_2SO_4

26   controlled the appearance of H_2SO_4-NH_3 clusters (#S > 3): All such clusters were observed when

27   [HOM]/[H_2SO_4] was smaller than 30. The number of H_2SO_4 molecules in the largest observable

28   cluster correlated with the probability of ion-induced nucleation (IIN) occurrence, which reached

29   almost 100 % when the largest observable cluster contained 6 or more H_2SO_4 molecules. During

30   selected cases when the time evolution of H_2SO_4-NH_3 clusters could be tracked, the calculated ion

31   growth rates exhibited a good agreement across measurement methods and cluster (particle) sizes. In

32   these cases, H_2SO_4-NH_3 clusters alone could explain ion growth up to 3 nm (mobility diameter). IIN

33   events also occurred in the absence of H_2SO_4-NH_3, implying that also other NPF mechanisms prevail

34   at this site, most likely involving HOMs. It seems that H_2SO_4 and HOMs both affect the occurrence

35   of an IIN event, but their ratio ([HOMs]/[H_2SO_4]) defines the primary mechanism of the event. Since

Atmospheric
Chemistry
and Physics
Discussions

36   that ratio is strongly influenced by solar radiation and temperature, IIN mechanism ought to vary

37   depending on conditions and seasons.

38

39   **1   Introduction**

40   Atmospheric aerosol particles are known to influence human health and the climate (Heal et al., 2012;

41   Stocker et al., 2013). New particle formation (NPF) from gas-phase precursors contributes to a major

42   fraction of the global cloud condensation nuclei population (Merikanto et al., 2009; Kerminen et al.,

43   2012; Gordon et al., 2017), and provides an important source of particulate air pollutants in many

44   urban environments (Guo et al., 2014).

45   Although NPF is an abundant phenomenon and has been observed in different places around the

46   globe within the boundary layer (Kulmala et al., 2004), the detailed mechanisms at each location may

47   differ and are still largely unknown. Experiments done in the CLOUD chamber (Cosmic Leaving

48   Outside Droplets) at CERN explored different NPF mechanisms on molecular level, including

49   sulfuric acid (H_2SO_4) and ammonia (NH_3) nucleation (Kirkby et al., 2011), H_2SO_4 and dimethylamine

50   (DMA) nucleation (Almeida et al., 2013), and pure biogenic nucleation (Kirkby et al., 2016) from

51   highly oxygenated organic molecules (HOMs) (Ehn et al., 2014). While chamber experiments can

52   mimic some properties of ambient observations (Schobesberger et al., 2013), it is still ambiguous to

53   what extent these chamber findings can be applied to understand NPF in the more complex

54   atmosphere, mostly due to the challenges in atmospheric measurements and characterization of the

55   nucleating species.

56   In the aforementioned chamber studies, ions have been shown to play a crucial role in enhancing new

57   particle formation, which is known as the ion-induced nucleation (IIN). The importance of IIN varies

58   significantly depending on the concentration and composition of the ion species, e.g., being negligible

59   in the H_2SO_4-DMA system (Almeida et al., 2013), moderate in the H_2SO_4-NH_3 system (Kirkby et al.,

60   2011) and dominating in the pure HOMs system (Kirkby et al., 2016). The recently developed

61   atmospheric-pressure-interface time-of-flight mass spectrometer (APi-TOF) (Junninen et al., 2010)

62   has been used for measuring ion composition at the SMEAR II station in Hyytiälä since 2009. Ehn et

63   al., (2010) have first shown that the negative ion population varied significantly, with H_2SO_4 clusters

64   dominating during the day and HOM-NO_3^- clusters during the night. This variation was further

65   studied by Bianchi et al., (2017), who grouped HOM-containing ions by separating the HOMs into

66   non-nitrate- and nitrate-containing species as well as into ion adducts with HSO_4^- or NO_3^- (Bianchi et

67   al., 2017). In the night time, HOMs may form negatively charged clusters containing up to 40 carbons

68   (Bianchi et al., 2017; Frege et al., 2018). In the daytime, H_2SO_4 and H_2SO_4-NH_3 clusters appear to

69 be the most prominent negative ions (Schobesberger et al., 2015; Schobesberger et al., 2013).

70 However, they have not yet been thoroughly studied regarding their appearance and their plausible

71 links to atmospheric IIN.

72 Although the fractional contribution of IIN to the total nucleation rate (J_{IIN}/J_{total}) turns out to be minor

73 in Hyytiälä (Kulmala et al., 2013, Manninen et al. 2010), its importance ought to vary along with the

74 temporal change in precursor vapor composition and concentration, which are reflected in the ion

75 compositions. This study aims to connect our current understandings of the contribution of IIN and

76 of ion composition to NPF, with a special focus on the fate of H_2SO_4-NH_3 clusters. We also extend

77 our analysis to ions other than H_2SO_4 clusters, i.e., HOMs, and identify their role in IIN, in addition

78 to other measured parameters on site. Finally, this study confirms the consistency between chamber

79 findings and atmospheric observations, even though it seems that at least two separate mechanisms

80 are alternatively controlling the IIN in Hyytiälä.

81

82 **2 Materials and Methods**

83 For this study, we used data collected at the Station for Measuring Forest Ecosystem-Atmospheric

84 Relations (SMEAR II station), in Hyytiälä, Southern Finland (Hari and Kulmala, 2005). In this study,

85 our data sets were obtained from intensive campaigns in 3 consecutive springs, 2011 – 2013. The

86 exact time periods of the APi-TOF measurements are 22nd of March until 24th of May 2011, 31st

87 March until 28th of April 2012, and 7th April until 8th of June 2013. For 134 days we were able to

88 extend our analysis to include: i) ion composition and chemical characterization using the APi-TOF

89 (Junninen et al., 2010), ii) particle and ion number size distribution using NAIS (e.g., Mirme and

90 Mirme 2013), iii) concentrations of H_2SO_4 and HOMs measured by the chemical ionization

91 atmospheric-pressure-interface time-of-flight mass spectrometer (CI-APi-TOF see, e.g., (Jokinen et

92 al., 2012;Ehn et al., 2014;Yan et al., 2016), and iv) other relevant parameters, e.g., NH_3 (Makkonen

93 et al., 2014), temperature and cloudiness (Dada et al., 2017).

94 2.1 Measurement of atmospheric ions

95 The composition of atmospheric anions was measured using the atmospheric-pressure-interface time-

96 of-flight mass spectrometer (APi-TOF) (Junninen et al., 2010). The instrument was situated inside a

97 container in the forest, direct sampling the air outside. To minimize the sampling losses, we firstly

98 drew the air at a larger flow rate within a wide tube (40 mm inner diameter), and another 30-cm-long

99 coaxial tube (10 mm outer diameter and 8 mm inner diameter) inside the wider one was used to draw

100 5 L/min towards the APi-TOF, 0.8 L/min out of which will enter through the pinhole. After entering

Atmospheric
Chemistry
and Physics
Discussions

Open Access

EGU

101   the pinhole, the ions are focused and guided through two quadrupoles and one ion lens, and finally

102   and detected by the time-of-flight mass spectrometer.

103   Different from the commonly used chemical-ionization mass spectrometer (CIMS), the APi-TOF

104   does not do any ionization, so it only measures the naturally charged ions in the sample. In the

105   atmosphere, the ion composition is affected by the proton affinity of the species: Molecules with the

106   lowest proton affinity are more likely to lose the proton and thus become negatively charged after

107   colliding many times with other species; similarly, molecules with the highest proton affinity would

108   probably become positively charged ions. In addition to the proton affinity, the neutral concentration

109   also plays a role in determining the ion composition by affecting the collision frequency. Due to the

110   limited ionization rate in the atmosphere, there is always a competition between different species in

111   taking the charges. For example, the H_2SO_4 often dominates the daytime spectrum in the daytime

112   when it is abundant, while in the night-time nitrate ions and its cluster with HOMs are always the

113   prominent due to the rare chance to collide with the H_2SO_4. Since the signal strength of an ion in APi-

114   TOF depends not only on the abundance of the respective neutral molecules, but also on the

115   availability of other charge-competing species, it is very important to note that APi-TOF can not

116   quantify the neutral species.

117   One important virtue of APi-TOF is that it does not introduce extra energy during sampling, which

118   ensures the sample is least affected when comparing to other measurement techniques such as CIMS.

119   although fragmentation cannot be fully avoided inside the instruments (Schobesberger et al., 2013).

120   Because of this, it is a best instrument to directly measure the composition of weakly bonded clusters

121   in the atmosphere.

122   The APi-TOF data were processed with the tofTools package (version 6.08) (Junninen et al., 2010).

123   Since the ion signal in APi-TOF is usually weak, a 5-hour integration time was used, after which the

124   signals of H_2SO_4-NH_3 clusters and HOMs were fitted (See Fig.1). For HOM signals, we used the

125   same peaks reported in Bianchi et al., (2017), and the total signal of HOM ions is the sum of all

126   identified HOMs.

127   It should also be mentioned that, the voltage tuning of the instrument was not the same in these years

128   we analyzed, which led to differences in the ion transmission efficiency function. For example, we

129   noticed that in 2011, the largest H_2SO_4-NH_3 clusters contained 6 clusters, whereas more than 10

130   H_2SO_4 in the clusters were observed in other years. This was very likely due to the very low ion

131   transmission in the mass range larger than about 700 Th. However, this should not affect our results

132   and conclusions, because clusters consisting of 6 H_2SO_4 molecules had little difference from larger

133   clusters in affecting the IIN (Fig. 3).

Atmospheric
Chemistry
and Physics
Discussions

134   2.2   Measurement of H_2SO_4 and HOMs

135   The concentrations of H_2SO_4 and HOMs were measured by the chemical ionization atmospheric-

136   pressure-interface time-of-flight mass spectrometer (CI-APi-TOF). The details of the quantification

137   method for H_2SO_4 can be found in Jokinen et al., (2012) and for HOMs in Kirkby et al., 2016. For all

138   data, we applied the same calibration coefficient (1.89×10^{10} 1/cm^3) reported by Jokinen et al., (2012).

139   Although the tunings of CI-APi-TOF were not exactly the same during the measurement period

140   included in this study, no systematic difference was found in the concentrations of H_2SO_4 and HOMs

141   from different years.

142   2.3   Measurements of ion and particle size distribution

143   The mobility distribution of charged particles and air ions in the range 3.2-0.0013 cm^{2}V^{-1}s^{-1}

144   (corresponding to mobility diameter 0.8 – 42 nm) were measured together with the size distribution

145   of total particles in the range ∼2.5 - 42 nm using a neutral cluster and air ion spectrometer (NAIS,

146   Airel Ltd., (Mirme and Mirme, 2013)). The instrument has two identical differential mobility

147   analyzers (DMA) which allow for the simultaneous monitoring of positive and negative ions. In order

148   to minimize the diffusion losses in the sampling lines, each analyzer has a sample flow rate of 30 L

149   min^{-1} and a sheath flow rate of 60 L min^{-1}. In "particle mode", when measuring total particle

150   concentration, neutral particles are charged by ions produced from a corona discharge in a "pre-

151   charging" unit before they are detected in the DMAs. The charging ions used in this process were

152   previously reported to influence the total particle concentrations below ∼2 nm (Asmi et al., 2008;

153   Manninen et al., 2010); for that reason, only the particle concentrations above 2.5 nm were used in

154   the present work. Also, each measurement cycle, i.e. 2 min in ion mode and 2 min in particle mode,

155   is followed by an offset measurement, during which the background signal of the instrument is

156   determined and then subtracted from measured ion and particle concentrations. In addition, particle

157   size distributions between 3 and 990 nm were measured with a differential mobility particle sizer

158   (DMPS) described in details in Aalto et al., (2001). Based on earlier work by Kulmala et al., (2001),

159   this data were used to calculate the condensation sink (CS), which represents the rate of loss of

160   condensing vapors on pre-existing particles.

161   2.4   Measurement of Meteorological parameter

162   The meteorological variables used as supporting data in the present work were measured on a mast,

163   all with a time resolution of 1 min. In specific, temperature and relative humidity were measured at

164   16.8 m using a PT-100 sensor and relative humidity sensors (Rotronic Hygromet MP102H with

165   Hygroclip HC2-S3, Rotronic AG, Bassersdorf, Switzerland), respectively. Global radiation was

166   measured at 18 m with a pyranometer (Middleton Solar SK08, Middleton Solar, Yarraville,

Atmospheric
Chemistry
and Physics
Discussions
Open Access
EGU

167   Australia), and further used to calculate the cloudiness parameter, as done previously by Dada et al.,

168   (2017, and references therein). This parameter is defined as the ratio of measured global radiation to

169   theoretical global irradiance, so that parameter values < 0.3 correspond to a complete cloud coverage,

170   while values > 0.7 are representative of clear sky conditions.

171

172   2.5   Calculation of particle formation rates and growth rates

173

174   The formation rates of 2.5 nm ions ($J_{2.5}^{+/-}$) and particles ($J_{2.5}$) were calculated using NAIS according

175   to Kulmala et al. (2012). In particular, $J_{2.5}$ was calculated using Eq. 1:

176    $$J_{2.5} = \frac{dN_{2.5-3.5}}{dt} + CoagS_{2.5} \times N_{2.5-3.5} + \frac{1}{1nm} GR_{1.5-3} \times N_{2.5-3.5}$$ Eq. 1

177   where $N_{2.5-3.5}$ is the particle concentration between 2.5 and 3.5 nm measured with the NAIS in particle

178   mode, $CoagS_{2.5}$ is the coagulation sink of 2.5 nm particles derived from DMPS measurements and

179    $GR_{1.5-3}$ is the particle growth rate calculated from NAIS measurements in ion mode. The calculation

180   of charged formation rates includes two additional terms to account for the loss of 2.5 – 3.5 nm ions

181   due to their recombination with sub-3.5 nm ions of the opposite polarity (fourth term of Eq. S2) and

182   the gain of ions caused by the attachment of sub-2.5 nm ions on 2.5-3.5 nm neutral clusters (fifth term

183   of Eq. 2):

184    $$J_{2.5}^{\pm} = \frac{dN_{2.5-3.5}^{\pm}}{dt} + CoagS_{2.5} \times N_{2.5-3.5}^{\pm} + \frac{1}{1nm} GR_{1.5-3} \times N_{2.5-3.5}^{\pm} + \alpha \times N_{2.5-3.5}^{\pm} N_{<3.5}^{\mp} - \beta \times N_{2.5-3.5} N_{<2.5}^{\pm}$$ Eq. S2

185   where $N_{2.5-3.5}^{\pm}$ is the concentration of positive or negative ions between 2.5 and 3.5 nm, $N_{<2.5}^{\pm}$ is the

186   concentration of sub-2.5 nm ions of the same polarity and $N_{<3.5}^{\mp}$ is the concentration of sub-3.5 nm

187   ions of the opposite polarity, all measured with the NAIS in ion mode. α and β are the ion-ion

188   recombination and the ion-neutral attachment coefficients, respectively, and were assumed to be

189   equal to 1.6×10^{-6} cm^3 s^{-1} and 0.01×10^{-6} cm^3 s^{-1}, respectively, according to Tammet and Kulmala

190   (2005).

191    $GR_{1.5-3}$ were calculated from NAIS data in ion mode using the "maximum" method introduced by

192   (Hirsikko et al., 2005). Briefly, the peaking time of the ion concentration in each size bin of the

193   selected diameter range was first determined by fitting a Gaussian to the concentration. The growth

194   rate was then determined by a linear least square fit through the times. The uncertainty in the peak

195   time determination was reported as the Gaussian's mean 67% confidence interval, and was further

196   taken into account in the growth rate determination.

Atmospheric
Chemistry
and Physics
Discussions

197   Similar approach was used to estimate the early growth rate of the H_2SO_4-NH_3 clusters detected with

198   the APi-TOF. Prior to growth rate calculation, we first converted cluster masses into diameters in

199   order to get growth rate values in nm h^{-1} instead of amu h^{-1}. For that purpose, we applied the

200   conversion from Ehn et al., (2011), using a cluster density of 1840 kg m^{-3}. The time series of the

201   cluster signals were then analysed in the same way as ion or particle concentrations using the

202   "maximum" method from Hirsikko et al. (2005), and the growth rate was calculated using the

203   procedure recalled above. Our ability to determine the early cluster growth rate from APi-TOF

204   measurement was strongly dependant on the strength of the signal of the different H_2SO_4-NH_3

205   clusters. As a consequence, the reported growth rates characterize a size range which might slightly

206   vary between the events, falling in a range between 1 and 1.7 nm.

207

208   **3   Results and Discussion**

209   **3.1   Daytime ion composition**

210   We examined the daytime ion composition of 134 days from three consecutive springs (2011-2013)

211   in Hyytiälä. Consistent with the findings by previous studies, showing that H_2SO_4 clusters are the

212   most abundant ions in the daytime (Ehn et al., 2010; Bianchi et al., 2017), we found that NH_3-free

213   H_2SO_4 clusters can contain up to three H_2SO_4 molecules when counting the HSO_4^- also as one H_2SO_4

214   molecule (($H_2SO_4)_2HSO_4^-$), and that NH_3 is always present in clusters containing 4 or more H_2SO_4

215   molecules. The latter feature suggests the important role of NH_3 as a stabilizer in growing H_2SO_4

216   clusters (Kirkby et al. 2011). NH_3-free clusters (at least dimers $H_2SO_4HSO_4^-$) were observed on 116

217   measurement days, but the signal intensity varied from day to day. Bigger clusters that contained NH_3

218   were observed on 39 days, containing a maximum of 4 to 13 H_2SO_4 per cluster. Figure 1 provides

219   four examples of daytime ion spectra, including an NH_3-free case (Fig. 1A) and three cases with a

220   different maximum size of H_2SO_4-NH_3 clusters (Fig. 1B-D), illustrating the significant variations in

221   signal and maximum size of H_2SO_4-NH_3 clusters. In the NH_3-free case, a larger number of HOM

222   clusters (green circles) was observed, indicating a competition between H_2SO_4 and HOMs in taking

223   the charges. The largest detected cluster during the measurement was $(H_2SO_4)_{12}(NH_3)_{13}HSO_4^-$, which

224   corresponds to a mobility-equivalent diameter of about 1.7 nm according to the conversion method

225   (Ehn et al., 2011) and is big enough to be detected by particle counters. Since the observed formation

226   of such large H_2SO_4-NH_3 clusters is essentially the initial step of IIN, we anticipate that the variation

227   of H_2SO_4-NH_3 clusters will influence the occurrence of IIN.

Atmospheric
Chemistry
and Physics
Discussions

228
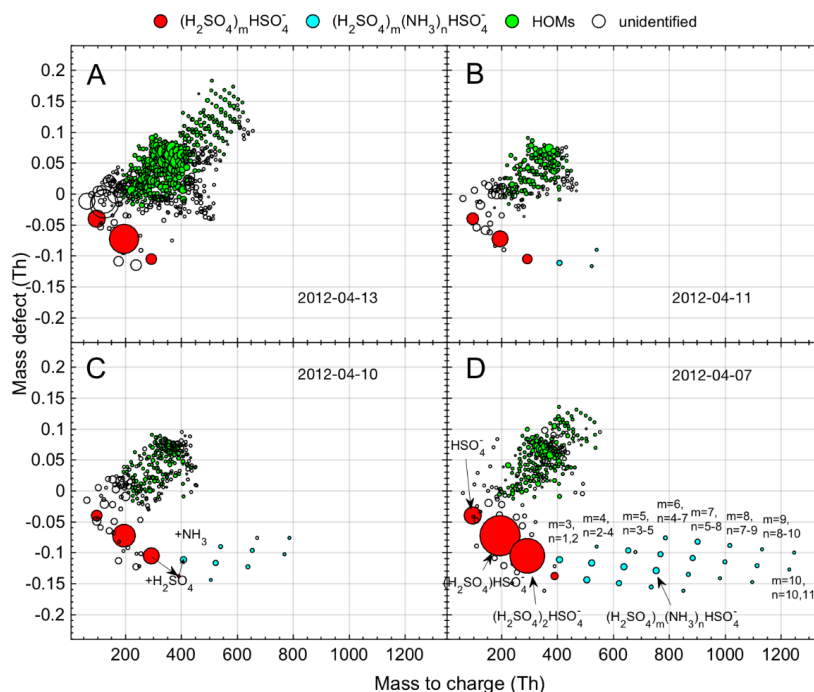
Figure 1 Mass defect plot showing the composition of ion clusters on four separate days. A) NH₃-free clusters,

B,C,D) H₂SO₄-NH₃ clusters with different maximum number of H₂SO₄ molecules. The circle size is linearly

proportional to the logarithm of the signal intensity.

3.2   The determining parameters for H_2SO_4-NH_3 cluster formation

To find out the dominating parameters that affect the formation of H_2SO_4-NH_3 clusters, we performed

a correlation analysis that included the ambient temperature, relative humidity (RH), wind speed,

wind direction, condensation sink (CS), as well as the gas-phase concentrations of NH_3, H_2SO_4, and

HOMs. Among all the examined parameters, we found that the ratio between concentrations of HOMs

and H_2SO_4 had the most pronounced influence on the appearance of H_2SO_4-NH_3 clusters. As shown

in Figure 2, all H_2SO_4-NH_3 clusters were detected when [HOMs]/[H_2SO_4] was smaller than 30. No

such dependence was observed for only [HOMs] or [H_2SO_4]. This implies that the appearance of

H_2SO_4-NH_3 clusters is primarily controlled by the competition between H_2SO_4 and HOMs in getting

the charges. More specifically, HSO_4^-, the main charge carrier in the daytime, may either collide with

neutral H_2SO_4 to form large clusters to accommodate NH_3, or collide with HOMs that prevents the

former process. In addition, a reasonable correlation was found between [HOMs]/[H_2SO_4] and

temperature, likely explained by emission of volatile organic compounds (VOC) increasing with

245   temperature, leading to higher HOMs concentrations, whereas the formation of H_2SO_4 is not strongly

246   temperature-dependent. This observation indicates that the formation of H_2SO_4-NH_3 clusters might

247   vary seasonally: we expect to see them more often in cold seasons when HOM concentrations are

248   low, and less often in warm seasons.

249   Parameters other than [HOMs]/[H_2SO_4] and temperature seemed to have little influence on the

250   formation of H_2SO_4-NH_3 clusters. Interestingly, we found that NH_3 was even lower when H_2SO_4-

251   NH_3 clusters were observed, indicating that the NH_3 concentration is not the limiting factor for

252   forming H_2SO_4-NH_3 clusters (also see section 3.4). In addition, H_2SO_4-NH_3 clusters were observed

253   in a wide range of RH spanning from 20 to 90 %, suggesting that RH is not affecting the cluster

254   formation. Besides, no clear influence from condensation sink (CS), wind speed, or wind direction

255   was observed.
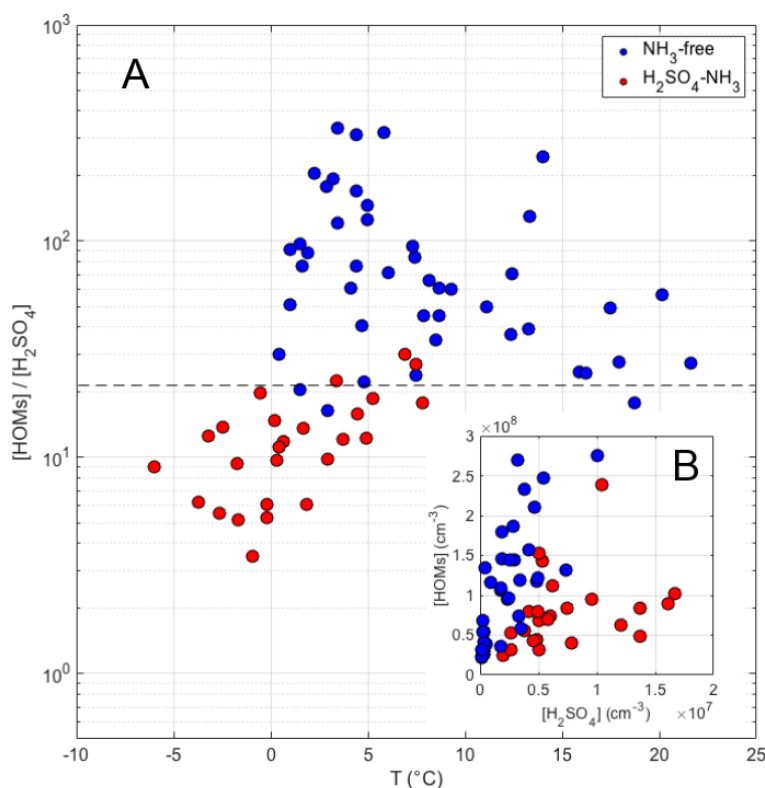
256

257   *Figure 2 The effect of concentration of HOMs, H_2SO_4, their ratio ([HOM]/[H_2SO_4]), and temperature on the*

258   *appearance of H_2SO_4-NH_3 clusters.*

259   3.3   **The relation between H_2SO_4-NH_3 clusters and IIN**

3.3.1 The effect of cluster size on the probability of IIN events

260

261 We identified IIN events using data from the NAIS (ion mode) by observing of an increase in the

262 concentration of sub-2 nm ions (Rose et al., 2018), and classified 67 IIN events out of the 134 days

263 of measurements. We defined the IIN probability as the number of days when IIN events were

264 identified out of the total number of days that were counted. For example, the overall IIN probably is

265 50 % (67 out of 134 days). We found that the maximum observed size of H_2SO_4-NH_3 clusters may

266 affect the occurrence of IIN. Our conclusion is complementary to previous theories which stated that

267 the critical step of particle nucleation is the formation of initial clusters that are big enough for

268 condensational growth to outcompete evaporation (Kulmala et al., 2013). To further understand the

269 size-dependency of IIN probability, we investigated the IIN probability when different maximum

270 sizes of H_2SO_4-NH_3 clusters were observed. As illustrated in Figure 3, the IIN probability increases

271 dramatically when larger H_2SO_4-NH_3 clusters were observed: IIN events were never observed when

272 only HSO_4^- or $H_2SO_4HSO_4^-$ were present, whereas the IIN probability increased to about 50 – 60 %

273 when the largest clusters contained 3 – 5 H_2SO_4 molecules. IIN occurred in 24 out of 25 days (96 %)

274 when the largest clusters consisted of no less than 6 H_2SO_4 molecules. Thus, it is evident that the

275 occurrence of IIN is related to the size and thus the stability of H_2SO_4-NH_3 clusters, and that a cluster

276 consisting of 6 H_2SO_4 molecules seems to lie on the threshold size of triggering nucleation.

277
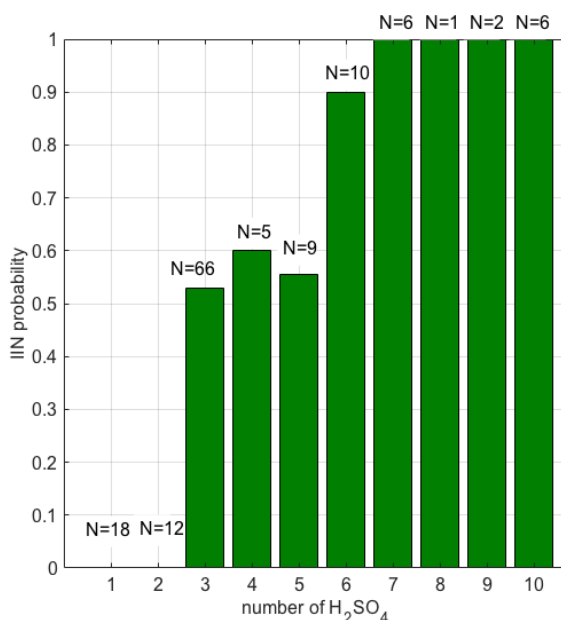
Figure 3 The maximum number of H$_2$SO$_4$ molecules observed in clusters and the respective IIN probability.

The days when it was unclear is IIN occurred was counted as non-event days. N denotes the number of days

when such clusters were the largest observed.

281   3.3.2   Continuous growth from clusters to 3 nm particles

282   Although the strong connection between the size of H$_2$SO$_4$-NH$_3$ clusters and the occurrence of IIN

283   was confirmed, it is challenging to directly observe the growth of these clusters in the atmosphere,

284   limited by the inhomogeneity of the ambient air and low concentrations of atmospheric ions.

285   Combining APi-TOF and NAIS measurements, we were however able to follow the very first steps

286   of the cluster growth for 8 of the detected events. In Figures 4A and 4B, we present two examples in

287   which the continuous growth of H$_2$SO$_4$-NH$_3$ clusters to 3 nm (mobility diameter) particles was

288   directly evaluated using the maximum-time method. The maximum times, determined from APi-TOF

289   and NAIS data independently, fall nicely on the same linear fit. The permanence of the growth and

290   the linearity of the fit suggests that the current mechanism (H$_2$SO$_4$-NH$_3$, acid-base) explains the

291   formation and growth of sub-3 nm ion clusters in these cases. In most cases, the calculation of cluster

292   GR from APi-TOF measurement suffered from high uncertainties, but a weak positive correlation

293   can be observed between the cluster growth rate and H$_2$SO$_4$ concentration (Fig. 4C). This correlation

294   is likely due to the collision of H$_2$SO$_4$ with existing H$_2$SO$_4$-NH$_3$ clusters being the limiting step for

295   cluster growth when NH$_3$ is abundant enough to follow up immediately (Schobesberger et al., 2015).

Atmospheric
Chemistry
and Physics
Discussions

296

297
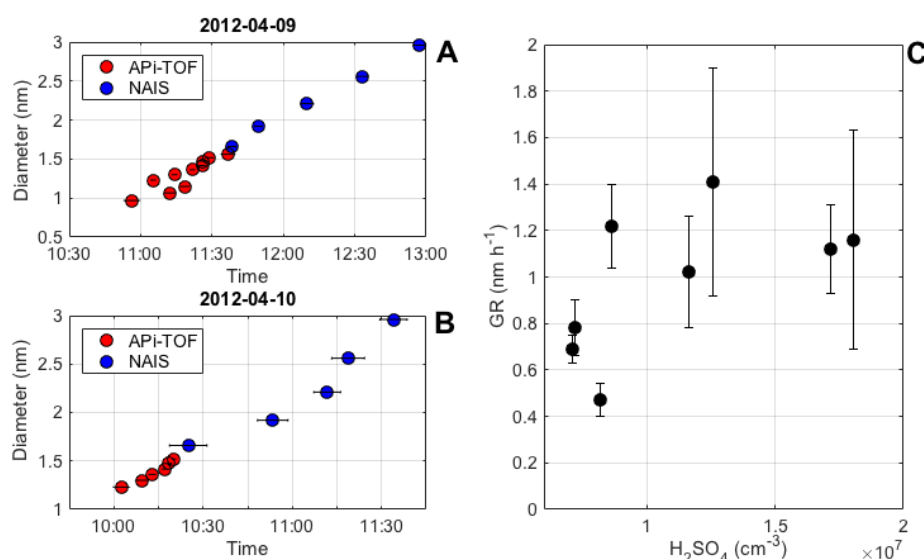
Figure 4 Cluster growth rate determined from APi-TOF (A) and NAIS (B) measurements using the maximum time method, and the correlation between growth rates and concentrations of H₂SO₄ molecules (C).

3.4   Evidence for other IIN mechanisms

For the 134 days of measurements, we were able to identify 67 IIN events using the NAIS data, out of which H_2SO_4-NH_3 clusters were observed on 32 days, implying that at least 35 IIN events were likely driven by mechanism(s) other than H_2SO_4-NH_3. In Figure 5, we classified the days according to the types of IIN observation: 32 IIN events involving H_2SO_4-NH_3 (SA-E), 3 non-events with the presence of H_2SO_4-NH_3 clusters (SA-NE), 35 IIN events involving other mechanisms (O-E), 41 other non-event days (O-NE), and 23 days with unclear types. We further present the respective statistics of additional measurements for the first four types of days, including the concentrations of plausible precursor vapors, condensation sink and meteorological parameters. It should be noted that the SA-NE has only 3 days, thus the statistics on this type of days might not be fully representative.

Consistent with the previous discussion (Fig. 2), low temperatures are conducive of IIN events via the H_2SO_4-NH_3 mechanism whilst being the highest other type of events (O-E) (Fig. 5A). The clear-sky parameter shows a noticeably higher value during both event types compared to the non-event cases (Fig. 5B), indicating that photo-chemistry related processes are important for all events. Moreover, the CS is obviously lower for both types of events than on non-event days (Fig. 5C). Although a strong effect on the appearance of H_2SO_4-NH_3 clusters has not been evidenced, it is a

12

316   most important parameter in regulating the occurrence of IIN. Similar effects of cloudiness and CS

317   on governing the occurrence of NPF have been reported by Dada et al., (2017) based on long-term

318   data sets.

319   Remarkably, NH_3 has very low concentrations during H_2SO_4-NH_3 events in comparison to other type

320   of events (Fig. 5D). This is likely due to high NH_3 concentrations coinciding with higher temperature

321   and thus elevated HOMs concentration, or the less stability of H_2SO_4-NH_3 clusters at high

322   temperatures that they fall apart to release NH_3 back to the atmosphere. This observation rules out

323   the addition of NH_3 as a limiting step in the H_2SO_4-NH_3 nucleation mechanism, but the participation

324   of NH_3 in other type of events cannot be excluded.

325   H_2SO_4 has the highest concentrations during the H_2SO_4-NH_3-involved events (Fig. 5E), but the

326   concentration of H_2SO_4 in SA-NE days is not much lower, suggesting that the occurrence of H_2SO_4-

327   NH_3-involved events is not solely controlled by the H_2SO_4 concentration. The Incorporating the effect

328   of CS ($[H_2SO_4]$/CS) significantly improves the separation (Fig.5F). HOM concentrations are highest

329   in the case of other events, revealing that HOMs play a key role in this mechanism (Fig. 5F), although

330   the contribution of H_2SO_4 in this HOM-involving IIN mechanism cannot be excluded. Similar to the

331   H_2SO_4-NH_3-driven cases, incorporating the CS better distinguishes the event and non-event cases.

332   Overall, our results suggest that the concentrations of H_2SO_4 and HOMs, together with the CS

333   governs the occurrence of IIN, whereas their ratio determines the exact underlying mechanism (Figs

334   2). Although H_2SO_4-NH_3 and HOMs clearly drives the SA-E and O-E events, respectively, we cannot

335   exclude the later participation of HOMs in SA-E cases or H_2SO_4 in O-E cases. Different NPF

336   mechanisms have also been identified at the Jungfraujoch station (*Bianchi et al.*, 2016 , *Frege et al.*,

337   2018) when influenced by different air masses. At SMEAR II station, on the other hand, our results

338   suggest that the natural variation of temperature is already sufficient to modify the NPF mechanism
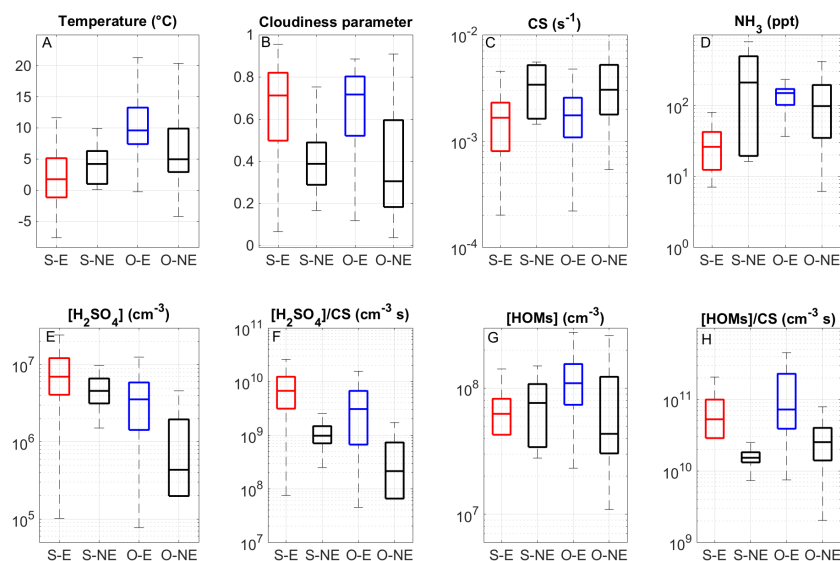
339   via modulating the biogenic VOC emissions.

Atmospheric
Chemistry
and Physics
Discussions

340

Figure 5 Comparison of different parameters for H_2SO_4-NH_3-involved events (SA-E, red bars), non-events
with the presence of H_2SO_4-NH_3 clusters (SA-NE, first column of black bars), other events (O-E, blue bars),
and other non-events (O-NE, second column of black bars).

3.5   Contribution of IIN to total nucleation rate

To further understand the respective importance of these mechanisms, we investigated particle
formation rate through ion-induced nucleation rate (J_{IIN}) and its contribution to the total formation
rate (J_{IIN}/J_{total}). We were able to calculate the J_{IIN} and J_{total} for 2.5 nm particles for 57 (out of 67) cases,
and the ratio J_{IIN}/J_{total} varied from 4 – 45 %, showing a clear correlation with the HOM ion signal (Fig.
6A). This indicate the participation of HOMs even in H_2SO_4-NH_3-driven cases. In addition, most of
the high J_{IIN}/J_{total} ratios were observed at moderate or low H_2SO_4 concentrations, e.g., J_{IIN}/J_{total} > 15 %
was only observed when $[H_2SO_4]$ < 6×10^6 cm^{-3}. These observations indicate that HOMs are
important in high J_{IIN}/J_{total} cases, while during events driven by H_2SO_4-NH_3 clusters low J_{IIN}/J_{total} is
more often observed. Accordingly, the median value of J_{IIN}/J_{total} for the H_2SO_4-NH_3 cases is about
12 %, consistent with Kulmala et al. (2013), but clearly higher (18 %) in HOM-driven events (Fig.
6D). Figures 6B and 6C reveal that both J_{IIN} and J_{total} values are in fact higher in H_2SO_4-NH_3 cases,
but the neutral nucleation pathway is relatively more enhanced, leading to the lower ratio. These
results suggest that ion-induced nucleation plays a more important role in the events driven by HOMs
than in the events driven by H_2SO_4-NH_3. A plausible explanation is that NH_3 is performing well in

359   stabilizing H_2SO_4 molecules during the clustering process, whereas ions are a relatively more

360   important stabilizing agent for HOM clustering.
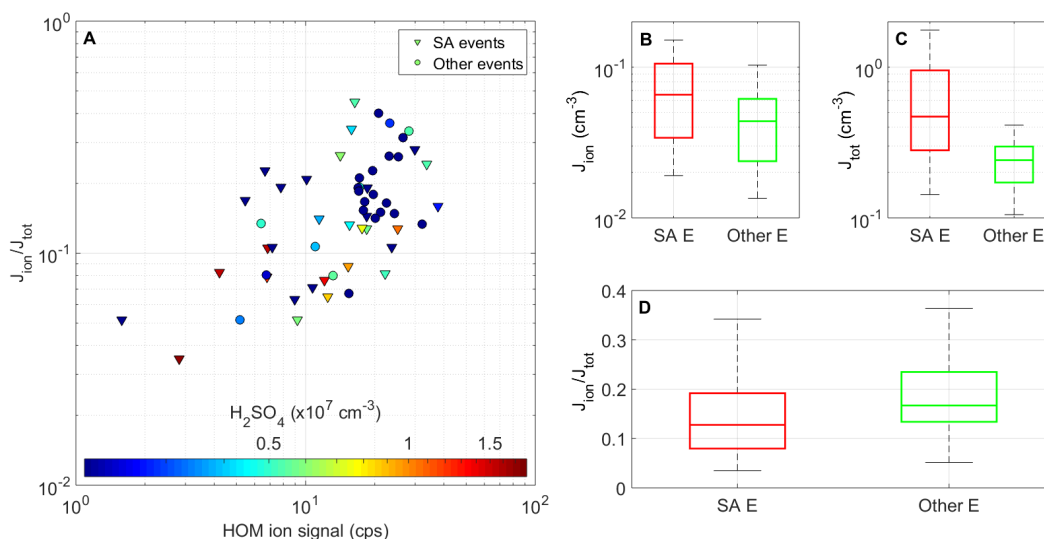
361

362   *Figure 6 Ion-induced nucleation rate and total nucleation rate under different nucleation mechanisms. A). The*
363   *fractional contribution of IIN to the total nucleation rate (J_{IIN}/J_{total}) as a function of total signal of HOM ions*
364   *color-coded by H_2SO_4 concentration. Data points are the averaged value from the starting time to the peaking*
365   *time of the 2.5 – 3.5 nm cluster concentration. B,C,D). Statistics of J_{IIN}, J_{total}, and J_{IIN}/J_{total} in the events driven*
366   *by different nucleation mechanisms.*

367

368   **4   Summary and Conclusion**

369   We investigated the formation of H_2SO_4-NH_3 anion clusters measured by APi-TOF during three

370   springs from 2011 to 2013 in a boreal forest in Southern Finland and their connection to IIN. The

371   abundancy and maximum size of H_2SO_4-NH_3 clusters showed great variability. Out of the total 134

372   measurement days, H_2SO_4-NH_3 clusters were only seen during 39 days. The appearance of these

373   clusters was mainly regulated by the concentration ratio between HOMs and H_2SO_4, which can be

374   changed by temperature via modulating the HOM production.

375   We found that the maximum observable size of H_2SO_4-NH_3 clusters has a strong influence on the

376   probability of an IIN event to occur. More specifically, when clusters containing 6 or more H_2SO_4

377   molecules were detected, IIN was observed at almost 100% probability. We further compared the

378   cluster ion growth rates from APi-TOF and NAIS using the maximum-time method. In these H_2SO_4-

379   NH_3 driven cases when we could robustly define the track of the cluster evolution, the cluster growth

380   was continuous and near linear from cluster-sizes up to 3 nm, suggesting co-condensation of H_2SO_4

381   and NH_3 as the sole growth mechanism. This does not exclude that organics could also participate in

382   the growth process in Hyytiälä in other days.

383   In addition, we noticed that there was another mechanism driving the IIN, and HOMs are the most

384   likely responsible species, although H_2SO_4 and NH_3 might also participate in this mechanism. Such

385   mechanism was at least responsible for 35 IIN events during the measurement days, and is expected

386   to be the prevailing one in higher-temperature seasons.

387   The contribution of IIN to the total rates of NPF differs between events driven by H_2SO_4-NH_3 and by

388   HOMs. IIN plays a bigger role in HOM-driven events, likely due to a relatively stronger stabilizing

389   effect of ions, contributing up to 40 % of the total nucleation rate. Since the production of HOMs and

390   H_2SO_4 are strongly modulated by solar radiation and/or temperature, a seasonal variation of IIN can

391   be expected, not only in terms of frequency, but also in terms of the underlying mechanisms, and

392   hence in terms of the enhancing effect of ions. This information should be considered in aerosol

393   formation modelling in future works.

394

395   Acknowledgement

402

403

404   Reference

405   Aalto, P., Hämeri, K., Becker, E., Weber, R., Salm, J., Mäkelä, J. M., Hoell, C., O'Dowd, C. D.,
406   Karlsson, H., and Hansson, H. C.: Physical characterization of aerosol particles during nucleation
407   events, *Tellus B*, 53, 344–358, 2001.

408
409   Almeida, J., Schobesberger, S., Kuerten, A., Ortega, I. K., Kupiainen-Maatta, O., Praplan, A. P.,
410   Adamov, A., Amorim, A., Bianchi, F., Breitenlechner, M., David, A., Dommen, J., Donahue, N. M.,
411   Downard, A., Dunne, E., Duplissy, J., Ehrhart, S., Flagan, R. C., Franchin, A., Guida, R., Hakala, J.,
412   Hansel, A., Heinritzi, M., Henschel, H., Jokinen, T., Junninen, H., Kajos, M., Kangasluoma, J.,
413   Keskinen, H., Kupc, A., Kurten, T., Kvashin, A. N., Laaksonen, A., Lehtipalo, K., Leiminger, M.,
414   Leppa, J., Loukonen, V., Makhmutov, V., Mathot, S., McGrath, M. J., Nieminen, T., Olenius, T.,
415   Onnela, A., Petaja, T., Riccobono, F., Riipinen, I., Rissanen, M., Rondo, L., Ruuskanen, T., Santos,
416   F. D., Sarnela, N., Schallhart, S., Schnitzhofer, R., Seinfeld, J. H., Simon, M., Sipila, M., Stozhkov,
417   Y., Stratmann, F., Tome, A., Troestl, J., Tsagkogeorgas, G., Vaattovaara, P., Viisanen, Y., Virtanen,
418   A., Vrtala, A., Wagner, P. E., Weingartner, E., Wex, H., Williamson, C., Wimmer, D., Ye, P., Yli-

Atmospheric
Chemistry
and Physics
Discussions

419   Juuti, T., Carslaw, K. S., Kulmala, M., Curtius, J., Baltensperger, U., Worsnop, D. R., Vehkamaki,
420   H., and Kirkby, J.: Molecular understanding of sulphuric acid-amine particle nucleation in the
421   atmosphere, *Nature*, 502, 359-363, 10.1038/nature12663, 2013.
422   Asmi, E., Sipil, M., Manninen, H. E., and Vanhanen, J.: Results of the first air ion spectrometer
423   calibration and intercomparison workshop, *Atmos. Chem. Phys. Discuss.,* 8, 3-7, 2008.
424
425   Bianchi, F., Garmash, O., He, X., Yan, C., Iyer, S., Rosendahl, I., Xu, Z., Rissanen, M. P., Riva, M.,
426   and Taipale, R.: The role of highly oxygenated molecules (HOMs) in determining the composition
427   of ambient ions in the boreal forest, *Atmos. Chem. Phys.*, 17, 13819-13831, 2017.
428
429   Dada, L., Paasonen, P., Nieminen, T., Buenrostro Mazon, S., Kontkanen, J., Peräkylä, O., Lehtipalo,
430   K., Hussein, T., Petäjä, T., and Kerminen, V.-M.: Long-term analysis of clear-sky new particle
431   formation events and nonevents in Hyytiälä, *Atmos. Chem. Phys.*, 17, 6227-6241, 2017.
432
433   Ehn, M., Junninen, H., Petäjä, T., Kurtén, T., Kerminen, V.-M., Schobesberger, S., Manninen, H.,
434   Ortega, I., Vehkamäki, H., and Kulmala, M.: Composition and temporal behavior of ambient ions in
435   the boreal forest, *Atmos. Chem. Phys*., 10, 8513-8530, 2010.
436
437   Ehn, M., Junninen, H., Schobesberger, S., Manninen, H. E., Franchin, A., Sipilä, M., Petäjä, T.,
438   Kerminen, V.-M., Tammet, H., and Mirme, A.: An instrumental comparison of mobility and mass
439   measurements of atmospheric small ions, *Aerosol Sci. Techno.*, 45, 522-532, 2011.
440
441   Ehn, M., Kleist, E., Junninen, H., Petäjä, T., Lönn, G., Schobesberger, S., Maso, M. D., Trimborn,
442   A., Kulmala, M., and Worsnop, D.: Gas phase formation of extremely oxidized pinene reaction
443   products in chamber and ambient air, *Atmos. Chem. Phys.*, 12, 5113-5127, 2012.
444
445   Ehn, M., Thornton, J. A., Kleist, E., Sipila, M., Junninen, H., Pullinen, I., Springer, M., Rubach, F.,
446   Tillmann, R., Lee, B., Lopez-Hilfiker, F., Andres, S. Y., 2016 #39}, Acir, I. H., Rissanen, M.,
447   Jokinen, T., Schobesberger, S., Kangasluoma, J., Kontkanen, J., Nieminen, T., Kurten, T., Nielsen,
448   L. B., Jorgensen, S., Kjaergaard, H. G., Canagaratna, M., Dal Maso, M., Berndt, T., Petaja, T.,
449   Wahner, A., Kerminen, V. M., Kulmala, M., Worsnop, D. R., Wildt, J., and Mentel, T. F.: A large
450   source of low-volatility secondary organic aerosol, *Nature*, 506, 476-480, 10.1038/nature13032,
451   2014.
452
453   Frege, C., Ortega, I. K., Rissanen, M. P., Praplan, A. P., Steiner, G., Heinritzi, M., Ahonen, L.,
454   Amorim, A., Bernhammer, A.-K., and Bianchi, F.: Influence of temperature on the molecular
455   composition of ions and charged clusters during pure biogenic nucleation, *Atmos. Chem. Phys.*, 18,
456   65-79, 2018.
457   Gordon, H., Kirkby, J., Baltensperger, U., Bianchi, F., Breitenlechner, M., Curtius, J., Dias, A.,
458   Dommen, J., Donahue, N. M., Dunne, E. M., Duplissy, J., Ehrhart, S., Flagan, R. C., Frege, C., Fuchs,
459   C., Hansel, A., Hoyle, C. R., Kulmala, M., Kürten, A., Lehtipalo, K., Makhmutov, V., Molteni, U.,
460   Rissanen, M. P., Stozhov, Y., Tröstl, J., Tsakogeorgas, G., Wagner, R., Williamson, C., Wimmer, D.,
461   Winkler, P. M., Yan, C., and Carslaw, K. S.: Causes and importance of new particle formation in the
462   present-day and preindustrial atmospheres. J. Geophys. Res. Atmos., 122, 8739-8760, 2017.

463   Guo, S., Hu, M., Zamora, M. L., Peng, J., Shang, D., Zheng, J., Du, Z., Wu, Z., Shao, M., and Zeng,
464   L.: Elucidating severe urban haze formation in China, *Proc. Natl. Acad. Sci.*, 111, 17373-17378,
465   2014.
466

Atmospheric
Chemistry
and Physics
Discussions

467   Hari, P., and Kulmala, M.: Station for measuring ecosystem-atmosphere relations, *Boreal Environ.*
468   *Res.*, 10, 315-322, 2005.

470   Heal, M., Kumar, P., and Harrison, R.: Particles, air quality, policy and health, *Chem. Soc. Rev.*, 41,
471   6606, 2012.

473   Hirsikko, A., Laakso, L., Hõrra, U., Aalto, P. P., Kerminen, V. M., and Kulmala, M.: Annual and size
474   dependent variation of growth rates and ion concentrations in boreal forest, *Boreal Environ. Res.*, 10,
475   Issue 5, 357-369, 2005.

477   Jokinen, T., Sipilä, M., Junninen, H., Ehn, M., Lönn, G., Hakala, J., Petäjä, T., Mauldin Iii, R.,
478   Kulmala, M., and Worsnop, D.: Atmospheric sulphuric acid and neutral cluster measurements using
479   CI-APi-TOF, *Atmos. Chem. Phys.*, 12, 4117-4125, 2012.

481   Junninen, H., Ehn, M., Petäjä, T., Luosujärvi, L., Kotiaho, T., Kostiainen, R., Rohner, U., Gonin, M.,
482   Fuhrer, K., and Kulmala, M.: A high-resolution mass spectrometer to measure atmospheric ion
483   composition, *Atmos. Meas. Tech.,* 3, 1039-1053, 2010.

485   Kerminen, V.-M., Paramonov, M., Anttila, T., Riipinen, I., Fountoukis, C., Korhonen, H., Asmi, E.,
486   Laakso, L., Lihavainen, H., Swietlicki, E., Svenningsson, B., Asmi, A., Pandis, S. N., Kulmala, M.,
487   and Petäjä, T.: Cloud condensation nuclei production associated with atmospheric nucleation: a
488   synthesis based on existing literature and new results, *Atmos. Chem. Phys.,* 12, 12037-12059, 2012,
489   https://doi.org/10.5194/acp-12-12037-2012, 2012.

491   Kirkby, J., Curtius, J., Almeida, J., Dunne, E., Duplissy, J., Ehrhart, S., Franchin, A., Gagné, S.,
492   Ickes, L., Kürten, A., Kupc, A., Met- zger, A., Riccobono, F., Rondo, L., Schobesberger, S.,
493   Tsagko- georgas, G., Wimmer, D., Amorim, A., Bianchi, F., Breitenlech- ner, M., David, A.,
494   Dommen, J., Downard, A., Ehn, M., Fla- gan, R. C., Haider, S., Hansel, A., Hauser, D., Jud, W.,
495   Junni- nen, H., Kreissl, F., Kvashin, A., Laaksonen, A., Lehtipalo, K., Lima, J., Lovejoy, E. R.,
496   Makhmutov, V., Mathot, S., Mikkilä, J., Minginette, P., Mogo, S., Nieminen, T., Onnela, A.,
497   Pereira, P., Petäjä, T., Schnitzhofer, R., Seinfeld, J. H., Sipilä, M., Stozhkov, Y., Stratmann, F.,
498   Tomé, A., Vanhanen, J., Viisanen, Y., Vrtala, A., Wagner, P. E., Walther, H., Weingartner, E.,
499   Wex, H., Win- kler, P. M., Carslaw, K. S., Worsnop, D. R., Baltensperger, U., and Kulmala, M.:
500   Role of sulphuric acid, ammonia and galac- tic cosmic rays in atmospheric aerosol nucleation,
501   Nature, 476, 429–433, https://doi.org/10.1038/nature10343, 2011.

502   Kirkby, J., Duplissy, J., Sengupta, K., Frege, C., Gordon, H., Williamson, C., Heinritzi, M., Simon,
503   M., Yan, C., Almeida, J., Tröstl, J., Nieminen, T., Ortega, I. K., Wagner, R., Adamov, A., Amorim,
504   A., Bernhammer, A.-K., Bianchi, F., Breitenlechner, M., Brilke, S., Chen, X., Craven, J., Dias, A.,
505   Ehrhart, S., Flagan, R. C., Franchin, A., Fuchs, C., Guida, R., Hakala, J., Hoyle, C. R., Jokinen, T.,
506   Junninen, H., Kangasluoma, J., Kim, J., Krapf, M., Kürten, A., Laaksonen, A., Lehtipalo, K.,
507   Makhmutov, V., Mathot, S., Molteni, U., Onnela, A., Peräkylä, O., Piel, F., Petäjä, T., Praplan, A.
508   P., Pringle, K., Rap, A., Richards, N. A. D., Riip- inen, I., Rissanen, M. P., Rondo, L., Sarnela, N.,
509   Schobesberger, S., Scott, C. E., Seinfeld, J. H., Sipilä, M., Steiner, G., Stozhkov, Y., Stratmann, F.,
510   Tomé, A., Virtanen, A., Vogel, A. L., Wag- ner, A. C., Wagner, P. E., Weingartner, E., Wimmer,
511   D., Winkler, P. M., Ye, P., Zhang, X., Hansel, A., Dommen, J., Donahue, N. M., Worsnop, D. R.,
512   Baltensperger, U., Kulmala, M., Carslaw, K. S., and Curtius, J.: Ion-induced nucleation of pure
513   biogenic parti- cles, Nature, 533, 521–526, https://doi.org/10.1038/nature17953, 2016.

514 Kulmala, M., Maso, M. D., Mäkelä, J. M., Pirjola, L., Väkevä, M., Aalto, P., Miikkulainen, P.,
515 Hämeri, K., and O'Dowd, C. D.: On the formation, growth and composition of nucleation mode
516 particles, *Tellus B*, 53, 479–490, 2001.

518 Kulmala, M., Vehkamäki, H., Petäjä, T., Dal Maso, M., Lauri, A., Kerminen, V.-M., Birmili, W., and
519 McMurry, P. H.: Formation and growth rates of ultrafine atmospheric particles: a review of
520 observations, *J. Aerosol Sci*, 35, 143-176, 2004.

522 Kulmala, M., Petäjä, T., Nieminen, T., Sipilä, M., Manninen, H. E., Lehtipalo, K., Dal, M. M., Aalto,
523 P. P., Junninen, H., and Paasonen, P.: Measurement of the nucleation of atmospheric aerosol particles,
524 *Nature Prot.*, 7, 1651, 2012.

526 Kulmala, M., Kontkanen, J., Junninen, H., Lehtipalo, K., Manninen, H. E., Nieminen, T., Petäjä, T.,
527 Sipilä, M., Schobesberger, S., Rantala, P., Franchin, A., Jokinen, T., Järvinen, E., Äijälä, M.,
528 Kangasluoma, J., Hakala, J., Aalto, P. P., Paasonen, P., Mikkilä, J., Vanhanen, J., Aalto, J., Hakola,
529 H., Makkonen, U., Ruuskanen, T., Mauldin, R. L., Duplissy, J., Vehkamäki, H., Bäck, J., Kortelainen,
530 A., Riipinen, I., Kurtén, T., Johnston, M. V., Smith, J. N., Ehn, M., Mentel, T. F., Lehtinen, K. E. J.,
531 Laaksonen, A., Kerminen, V.-M., and Worsnop, D. R.: Direct Observations of Atmospheric Aerosol
532 Nucleation, *Science*, 339, 943-946, 10.1126/science.1227385, 2013.

534 Makkonen, U., Virkkula, A., Hellen, H., Hemmila, M., Sund, J., Aijala, M., Ehn, M., Junninen, H.,
535 Keronen, P., and Petaja, T.: Semi-continuous gas and inorganic aerosol measurements at a boreal
536 forest site, *Boreal Environ. Res.*, 2014.

537 Manninen, H. E., Nieminen, T., Asmi, E., Gagne, S., Hakkinen, S., Lehtipalo, K., Aalto, P., Vana,
538 M., Mirme, A., Mirme, S., Horrak, U.,   Plass-Dulmer, C., Stange, G., Kiss, G., Hoffer, A., Toeroe,
539 N., Moerman, M., Henzing, B., de Leeuw, G., Brinkenberg, M., Kouvarakis , G. 55 N., Bougiatioti,
540 A., Mihalopoulos, N., O'Dowd, C., Ceburnis, D., Arneth, A., Svenningsson, B., Swietlicki, E.,
541 Tarozzi, L., Decesari, S., Facchini, M. C., Birmili, W., Sonntag, A., Wiedensohler, A., Boulon, J.,
542 Sellegri, K., Laj, P ., Gysel, M., Bukowiecki, N., We ingartner, E., Wehrle, G., Laaksonen, A., Hamed,
543 A., Joutsensaari, J., Petaja, T., Kerminen, V. M., and Kulmala, M.: EUCAARI ion spectrometer
544 measurements at 12 European sites - analysis of new particle formation events, Atmos Chem Phys,
545 10, 7907-7927, 10.5194/acp-10-7907- 2010, 2010.

546 Merikanto, J., Spracklen, D., Mann, G., Pickering, S., and Carslaw, K.: Impact of nucleation on global
547 CCN, *Atmos. Chem. Phys.*, 9, 8601-8616, 2009.

548 Mirme, S., and Mirme, A.: The mathematical principles and design of the NAIS-a spectrometer for
549 the measurement of cluster ion and nanometer aerosol size distributions, *Atmos. Meas. Tech.*, 6, 1061,
550 2013.

552 Riccobono, F., Schobesberger, S., Scott, C. E., Dommen, J., Ortega, I. K., Rondo, L., Almeida, J.,
553 Amorim, A., Bianchi, F., and Breitenlechner, M.: Oxidation products of biogenic emissions
554 contribute to nucleation of atmospheric particles, *Science*, 344, 717-721, 2014.

556 Rose, C., Zha, Q., Dada, L., Yan, C., Lehtipalo, L., Junninen, H., Buenrostro Mazon, S., Jokinen, T.,
557 Sarnela, N., Sipilä, M., Petäjä, T., Kerminen, V.-M., Bianchi, F., Kulmala, M.: observations of
558 biogenic ion-induced cluster formation in the atmosphere, *in prep*.

Atmospheric
Chemistry
and Physics
Discussions

560   Schobesberger, S., Junninen, H., Bianchi, F., Lönn, G., Ehn, M., Lehtipalo, K., Dommen, J., Ehrhart,
561   S., Ortega, I. K., and Franchin, A.: Molecular understanding of atmospheric particle formation from
562   sulfuric acid and large oxidized organic molecules, *Proc. Natl. Acad. Sci.*, 110, 17223-17228, 2013.
563
564   Schobesberger, S., Franchin, A., Bianchi, F., Rondo, L., Duplissy, J., Kürten, A., Ortega, I., Metzger,
565   A., Schnitzhofer, R., and Almeida, J.: On the composition of ammonia–sulfuric-acid ion clusters
566   during aerosol particle formation, *Atmos. Chem. Phys.*, 15, 55-78, 2015.
567
568   Stocker, T., Qin, D., Plattner, G., Tignor, M., Allen, S., Boschung, J., Nauels, A., Xia, Y., Bex, B.,
569   and Midgley, B.: IPCC, 2013: climate change 2013: the physical science basis. Contribution of
570   working group I to the fifth assessment report of the intergovernmental panel on climate change,
571   2013.
572
573   Tammet, H., and Kulmala, M.: Simulation tool for atmospheric aerosol nucleation bursts, *J. Aerosol
574   Sci.*, 36, 173-196, 2005.
575   Yan, C., Nie, W., Aijala, M., Rissanen, M. P., Canagaratna, M. R., Massoli, P., Junninen, H., Jokinen,
576   T., Sarnela, N., Hame, S. A. K., Schobesberger, S., Canonaco, F., Yao, L., Prevot, A. S. H., Petaja,
577   T., Kulmala, M., Sipila, M., Worsnop, D. R., and Ehn, M.: Source characterization of highly oxidized
578   multifunctional compounds in a boreal forest environment using positive matrix factorization, *Atmos.
579   Chem. Phys.*, 16, 12715-12731, 10.5194/acp-16-12715-2016, 2016
580